Cell Stem Cell
Article

A Hierarchical Network Controls Protein Translation during Murine Embryonic Stem Cell Self-Renewal and Differentiation

Prabha Sampath,[1,2] David K. Pritchard,[1] Lil Pabon,[1,2] Hans Reinecke,[1,2] Stephen M. Schwartz,[1] David R. Morris,[3,*] and Charles E. Murry[1,2,*]
[1]Department of Pathology, Center for Cardiovascular Biology
[2]Institute for Stem Cell and Regenerative Medicine
University of Washington, Seattle, WA 98109, USA
[3]Department of Biochemistry, University of Washington, Seattle, WA 98195, USA
*Correspondence: dmorris@u.washington.edu (D.R.M.), murry@u.washington.edu (C.E.M.)
DOI 10.1016/j.stem.2008.03.013

SUMMARY

Stem cell differentiation involves changes in transcription, but little is known about translational control during differentiation. We comprehensively profiled gene expression during differentiation of murine embryonic stem cells (ESCs) into embryoid bodies by integrating transcriptome analysis with global assessment of ribosome loading. While protein synthesis was parsimonious during self-renewal, differentiation induced an anabolic switch, with global increases in transcript abundance, polysome content, protein synthesis, and protein content. Furthermore, 78% of transcripts showed increased ribosome loading, thereby enhancing translational efficiency. Transcripts under exclusive translational control included the transcription factor ATF5, the tumor suppressor DCC, and the β-catenin agonist Wnt1. We show that a hierarchy of translational regulators, including mTOR, 4EBP1, and the RNA-binding proteins DAZL and GRSF1, control global and selective protein synthesis during ESC differentiation. Parsimonious translation in pluripotent state and hierarchical translational regulation during differentiation may be important quality controls for self-renewal and choice of fate in ESCs.

INTRODUCTION

Murine embryonic stem cells (ESCs) can be maintained as permanent, undifferentiated cell lines (Smith et al., 1988; Williams et al., 1988). Upon withdrawal of the cytokine leukemia inhibitory factor (LIF), they can be induced to differentiate into spheroidal cell aggregates termed embryoid bodies (EBs) (Bain et al., 1995). Understanding the crucial molecular switches that regulate early ESC differentiation would provide insights into early development, as well as enhance the potential of these interesting cells in therapeutic applications (Ali et al., 2002; Bader et al., 2000; Chinzei et al., 2002).

Cellular differentiation is modeled as a network of regulatory circuits that direct multiple steps of gene expression and mediate spatiotemporal control of a cell's proteome, in the process determining both cellular phenotype and plasticity. ESC differentiation is known to involve modulation of transcription of a vast number of genes (Dvash et al., 2004; Gunji et al., 2004; Pritsker et al., 2006; Ramalho-Santos et al., 2002). Although traditional microarray analysis has provided valuable insight into the temporal appearance and disappearance of individual mRNAs, it is mRNA translation that ultimately determines the cell's proteome. Multiple studies indicate that translational control mechanisms can contribute to proteome composition by finely tuning gene expression in oocytes and in differentiating adult cells (Gray and Wickens, 1998; Potireddy et al., 2006; Pradet-Balade et al., 2001); however, translational control during ESC differentiation is not yet characterized.

Translation state array analysis (TSAA) is a genome-scale approach that allows assessment of the impact of translation on gene expression by combining sucrose gradient centrifugation (for separation of polyribosome complexes from ribosome-free transcripts or inactive mRNP particles) with microarray analysis (Arava, 2003; Arava et al., 2003; MacKay et al., 2004; Pradet-Balade et al., 2001; Preiss et al., 2003; Serikawa et al., 2003; Zong et al., 1999). In this approach, changes in ribosome loading are assayed on a genome-wide scale and serve as indicators of the efficiencies at which the individual transcripts are translated. We used TSAA to measure both transcript abundance and ribosome loading during ESC differentiation. Undifferentiated ESCs are found to be relatively polysome poor, as the result of inefficient loading of most transcripts with ribosomes. Differentiation is accompanied by a global increase in both transcript levels and efficiency of protein translation. Multiple vital genes were identified where protein levels are exclusively regulated at the translational level during differentiation. Translational activation appears to proceed through a hierarchy of translational regulators, including mTOR, DAZL and GRSF1, that ensure appropriate gene expression and control murine ESC differentiation.

RESULTS

To obtain enriched populations of cells from two distinct cellular states, we compared day 0 undifferentiated ESCs and day 5

differentiated EBs. The 5 day time point was chosen based on the expression profiles of SSEA-1 and Oct4, two well-characterized markers for the pluripotent state. As shown in the Supplemental Data available online, LIF removal does not lead to the immediate downregulation of SSEA-1 and Oct4. Instead, we observe a gradual decrease in expression. Only ~5% of cells were SSEA-1$^+$ by day 5, indicating that biochemical samples prepared at this time would not be significantly contaminated by undifferentiated cells (Supplemental Data).

ESCs Globally Elevate Protein Synthesis during Differentiation

Electron microscopy revealed that over the first 5 days of differentiation ESCs increased their content of Golgi apparatus and rough endoplasmic reticulum, consistent with increased protein synthesis (Figures 1A and 1B, [a]–[c]). Concomitantly, the cytoplasmic volume increased, resulting in an ~50% increase in cytoplasm:nuclear area (Figure 1C). Total RNA content and total protein content of cells was elevated ~1.5-fold and 1.3-fold respectively, over the same period of time (Figures 1E and 1F), also consistent with increased protein synthesis. Ribosomal RNA (rRNA) content showed only an ~20% increase (Figure 1G), suggesting other RNA subtypes contributed to the 50% increase in total RNA. To assess the rates of protein synthesis, cells were labeled for 3 hr with [^{35}S]methionine and cytoplasmic lysates were subjected to SDS-PAGE and visualized by autoradiography (Figure 1H). The autoradiographic patterns indicate ~2-fold higher [^{35}S]methionine incorporation rate in EBs compared to ESCs (Figure 1I). These ultrastructural and biochemical changes point to a general increase in the rate of protein synthesis during ESC differentiation. The increase in protein synthesis rates could be due to an increase in transcript abundance, an increase in translational efficiency, or both.

Increased Polysome Content during Differentiation

As one measure of global translational activity during differentiation, cytoplasmic lysates from ESCs and EBs were fractionated by sucrose gradient centrifugation. This separated free mRNP particles and polyribosomes according to size. Inspection of the A_{254} profiles across the sucrose gradients reveals a significant increase in absorbance in the polysome region of the EB extracts (Figure 2A). Polysome profiles were quantitated by calculating the percent area beneath the polysomal fractions (pool-3) with respect to the total area under the curve using Image Pro analysis. Quantification demonstrated that the polysome region increased from ~25% of total area under the absorbance curve in the ESCs to 41% of total area in EBs (Figure 2B). This 1.6-fold increase in ribosome-associated messages is consistent with the elevated protein synthetic rate and cellular protein content observed during the differentiation of ESC into EBs (Figures 1H and 1I).

ESCs Globally Elevate Transcript Levels during Differentiation

To obtain total transcript levels in ESCs versus EBs, microarrays were used to interrogate the transcript composition of unfractionated cell lysates. Total unfractionated RNA from ESCs and EBs was hybridized to Affymetrix arrays. Signal intensity was normalized using spike-in bacterial control RNA, added prior to RNA isolation, to control for variation in the efficiency of RNA extraction and probe synthesis. After intensity filtering and removal of redundant probe sets, we obtained a list of 5828 expressed genes. On average, we observed 1.4-fold greater probe hybridization intensity in EBs versus ESCs. Interestingly, 5688 genes (97%) showed statistically significant differential expression between ESCs and EBs at multiple testing adjusted $p < 0.05$. These data suggest that a global increase in mRNA on a per-cell basis contributes to the increase in total RNA measured biochemically.

A graphic representation of differential gene expression using a scatter plot shows the relationship between mean ratio change between EB and ESC transcripts (vertical axis) and the average intensity of expression (horizontal axis) of the 5828 expressed genes on the array (Figure 3A). This demonstrates a population shift above the line of unity, consistent with globally increased transcript levels. To ensure that this apparent global upregulation of transcript levels did not result from errors in array normalization, 30 genes were selected for verification by quantitative RT-PCR (qRT-PCR) using an internally spiked-in standard (luciferase mRNA) to correct for RNA recovery and efficiency of reverse transcription. This revealed an excellent linear correlation between array and qRT-PCR ($r^2 = 0.96$), with a line passing through the origin and a slope not significantly different from 1.0 (Figure 3B). These results demonstrate a global increase in transcript abundance in the differentiated ESC progeny.

Transcriptome-wide Analysis of Ribosome Loading

To measure changes in translational efficiency across the transcriptome, undifferentiated ESCs and day 5 EBs were subjected to polysome fractionation via sucrose gradient centrifugation. Four pools were prepared from the resulting 12 fractions (Figure 2A) based on ribosome loading. Pool 1 contains mRNP particles and ribosomal subunits. Pool 2 contains single ribosomes and mRNA species with 2 to 3 attached ribosomes. Transcripts could occur in this region as a result of either inefficient translation or short transcript length. Pool 3 consists of transcripts with four or more attached ribosomes, and we have defined this region as the well-translated pool. Pool 4 contains transcripts that sediment very rapidly, due either to many attached ribosomes or to association with other large bodies such as organelles, granules, cytoskeleton, or membranes. RNA isolated from the four pools was subjected to microarray analysis as described for the unfractionated RNA, again using spike-in bacterial control RNA. As before, the analysis was restricted to intensity-filtered probe sets as described in the Experimental Procedures.

The percentage of a given transcript's association with pool 3 was used as an index of ribosome loading. Using this approach, transcripts from EBs showed a general elevation of ribosome loading relative to the mRNAs from ESCs (Figures 3C and 3D). Of the 5828 genes in the filtered sample, 4559 showed statistically significant ($p < 0.05$, multiple testing adjusted) changes in polysome association. The median ratio change of differential translation for the statistically significant genes was 1.54, indicating that most genes showed at least a 1.5-fold increase in ribosome loading during differentiation. Conversely, almost none of the genes showed a significant decrease in ribosome association. To validate the array-based ribosome loading data, the

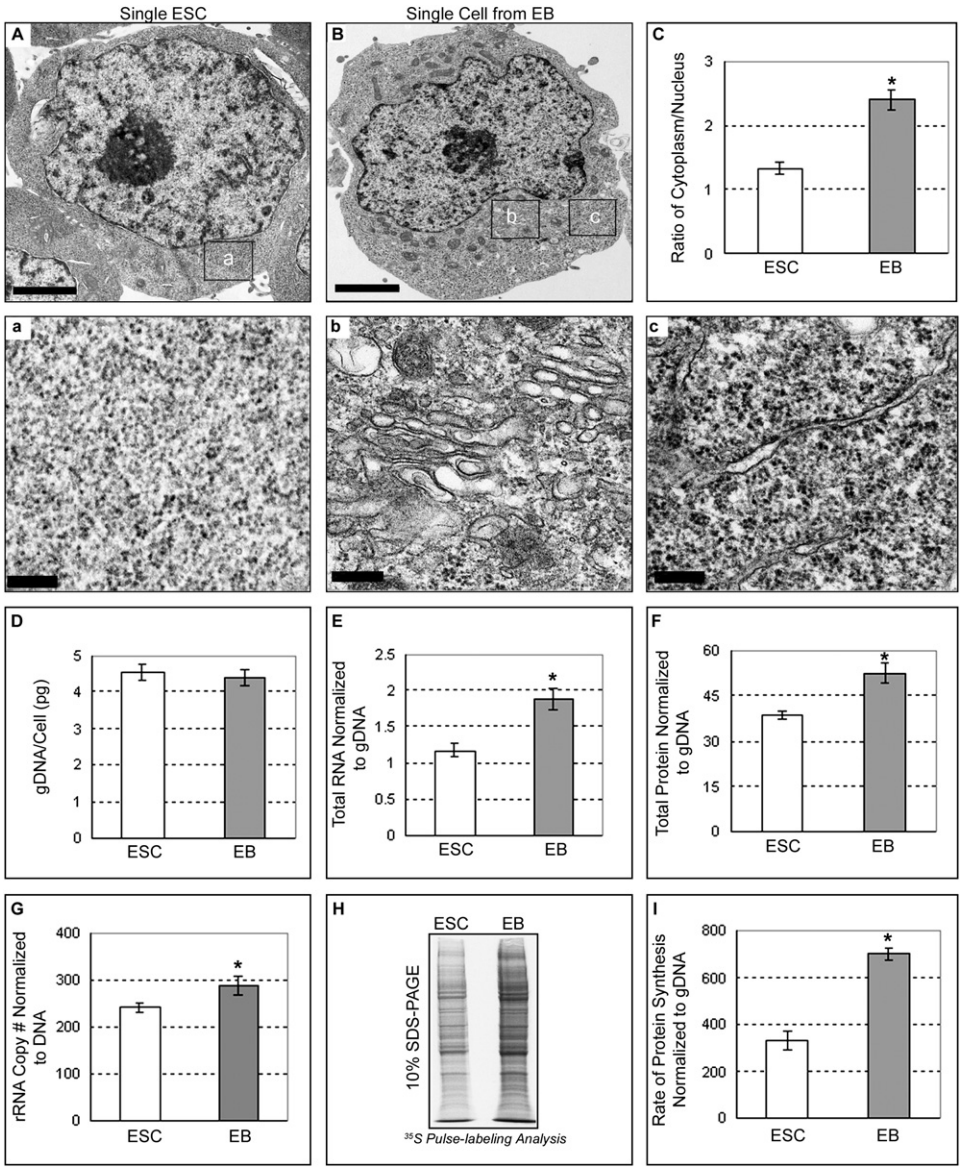

Figure 1. Increased Protein Synthesis in EBs versus ESCs

(A–C) (A and B) Transmission electron micrographs (TEM) of a single ESC and a single cell from EBs. The left panel (A) depicts an undifferentiated mouse ESC, and the middle panel (B) depicts its day 5 differentiated progeny. (C) Cytoplasm to nuclear area ratios in ESCs versus EBs. Morphometry of TEM images reveals a higher cytoplasmic to nuclear ratio in EBs compared to the ESCs. (a) High-power photomicrograph of the undifferentiated ESC. (b and c) Panels show higher magnifications of (B). Note the cytoplasm highlighting the abundance of Golgi bodies (b) and rough ER (c) in the differentiated progeny compared to its undifferentiated state. Scale bars represent 2 μm (A and B) and 200 nm (a–c), respectively.

(D–G) Quantification of biochemical parameters in the ESCs and EBs. The DNA content per cell did not change during differentiation (D). In contrast, total RNA (E) and total protein (F) normalized to gDNA were higher in EBs compared to ESCs. Ribosomal RNA content normalized to DNA showed only a modest increase in EBs (G).

(H and I) Quantification of protein synthesis rates using [^{35}S]methionine. SDS-PAGE was performed with equal amounts of [^{35}S]-radiolabeled protein followed by autoradiography and phosphorimage analysis. An ~2-fold greater amino acid incorporation was observed in EBs. Statistical significance ($p < 0.05$) for all measurements was determined by two-tailed student's t test, assuming unequal variance.

abundance of 30 selected transcripts was validated by qRT-PCR. The array and qRT-PCR data showed a good direct correlation ($R^2 = 0.72$) (Figure 3D), indicating that the array profiles can be used to ascertain global and specific properties of translation. Validation of our strategy of merging the 12 polysome fractions into four pools is presented below (Figures 4A and 4B).

Transcriptome-wide Comparison of Abundance and Ribosome Loading

When we plot the EB/ESC translational efficiency ratio versus transcript abundance ratio on an XY scatter plot, four distinct groups emerge: (1) transcripts displaying statistically significant changes in both abundance and translational efficiency

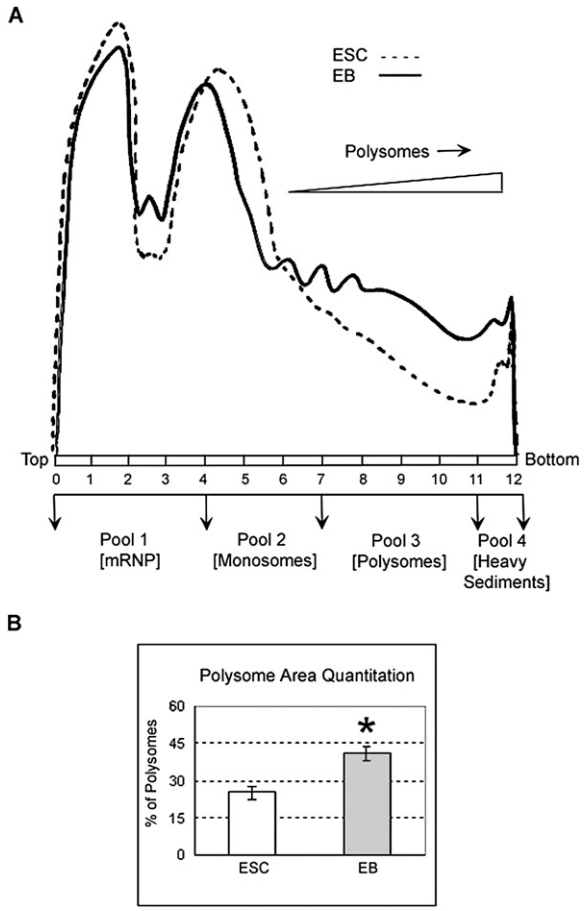

Figure 2. Increased Ribosome Loading upon Differentiation

(A) Comparison of polysome profiles. Lysates from ESCs and EBs were subjected to sucrose gradient density centrifugation. Gradients were collected in 12 fractions and, for some experiments, pooled into four groups as indicated. The differentiated EBs contained much more RNA in the polysome fraction, indicating a global upregulation of protein synthesis.

(B) Quantification of the area under the curve for polysomal region (pool 3) as a percentage of the total area. Note that the EBs (*$p < 0.05$) show a 1.6-fold increase in the polysomal area compared to the ESCs.

(representing 76% of expressed transcripts; Figure 3E, light blue dots; Table 1); (2) transcripts displaying statistically significant changes in abundance with no change in translational efficiency (21% of transcripts; Figure 3E, pink dots; Table 1); (3) transcripts showing no change in abundance but statistically changed translation states (2% of transcripts; Figure 3E, orange dots; Table 1); and (4) transcripts changing in neither abundance nor translational efficiency during this cellular transition (1% of transcripts; Figure 3E, dark blue dots). (Note that only seven transcripts showed reduced transcription and unchanged translation, while none of the transcripts with an intensity cutoff of A > 6 showed significant decreases in translational efficiency.)

To test whether the observed correlation affects only a subclass of functional groups or reflects a more general regulatory coupling, changes in transcript abundance and translation state were analyzed after subdivision of genes into functional groups using GOSTAT (Beissbarth and Speed, 2004). Statistically filtered genes with transcript abundance changes of ±2-fold or greater were subjected to gene ontology (GO) analysis. Further, within these GO groups the translational score was analyzed. Transcripts grouped based on molecular function using GOSTAT included a few general broad categories like DNA binding, RNA binding, ion binding, and more specific GO categories like transcription factors, translation initiation factors, and ribosomal constituents. Despite extensive evaluation by GO analysis, we did not detect discrete functional groupings of genes based on combined transcription and translation state analysis. This suggests that the changes observed in 5-day-old EBs reflect a global process.

Polysome Profiles of Selected Transcripts

We used qRT-PCR to compare the distribution of specific transcripts in each of the 12 fractions from sucrose gradients to the predictions made using pooled samples from translation state array analysis. In every case, the high-resolution polysome profile matched the transcript's predicted distribution from the pooled samples (Figures 4A and 4B). This validates the pooling strategy (Figure 2A) used in assigning transcripts into poorly translated and well-translated states.

Several of these genes merit specific attention. DAZL, thought to be specific to germ cells, is involved in regulation of mRNA translation (Collier et al., 2005). DAZL showed marked increases in both transcription and translation efficiency, and it could potentially be involved in the global upregulation of translation during ESC differentiation (Figure 4A). B-Myb, a transcription factor that promotes cell-cycle activation through interaction with E2F and Rb family members (Joaquin and Watson, 2003), also showed increased transcript levels and translational efficiency. On the other hand, SOCS3, a regulator of LIF-dependent signaling (Forrai et al., 2006), showed a marked decrease in transcript abundance but no change in translational efficiency.

The TSAA performed here allowed identification of 104 transcripts that display increased protein levels in the absence of transcriptional upregulation, that is, exclusively under translational control. ATF5 is a transcription factor implicated in neural development, regulating fate choices among neuron versus astrocytic lineages (Angelastro et al., 2003, 2005). Deleted in colon cancer (DCC) is a receptor for the netrin family of ligands involved in axonal guidance (Llambi et al., 2001). In ESCs, ATF5 and DCC mRNA sedimented in fractions corresponding to ribonucleoprotein (RNP) particles and monosomes, consistent with poor translation of both transcripts (Figure 4B). Following differentiation, ATF5 and DCC mRNA shifted to higher-order fractions, corresponding to polysome-loaded mRNAs, suggesting active translation (Figure 4B). However, in ESCs ribosome loading of ATF5 and DCC mRNAs is prevented.

Wnt1 is an activator of the β-catenin pathway involved in regulation of pluripotency and multiple areas of development (Cai et al., 2007; Katoh and Katoh, 2007). Wnt1 was one of the rare transcripts identified as showing decreased translational efficiency during differentiation by array analysis. When we examined individual fractions, we found that, in ESCs, Wnt1 sediments in higher-order fractions corresponding to polysome-loaded mRNAs. This suggests active translation. Following differentiation, Wnt1 sediments in fractions of the gradient corresponding with RNP particles and monosomes (Figure 4B). This indicates that, although there is no overall change in Wnt1

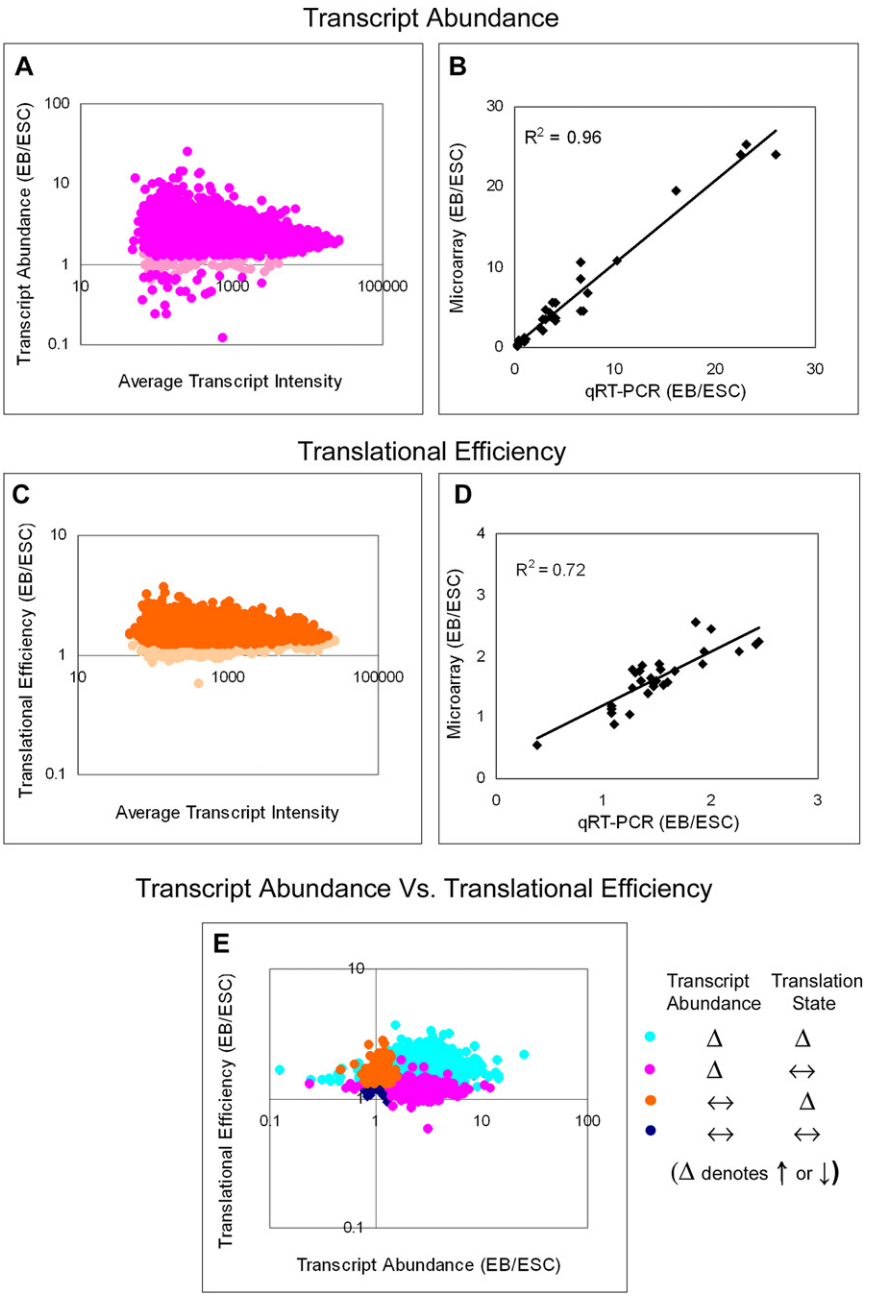

Figure 3. Global Upregulation of Transcript Abundance and Translation State during ESC Differentiation

(A) Global upregulation of transcription during ESC differentiation. The vertical axis depicts the ratio of transcript abundance in EBs versus ESCs (unfractionated samples). The horizontal axis represents mean abundance ([ESC + EB] / 2) of individual transcripts. Dark pink dots represent transcripts that show statistically significant differential expression (*$p < 0.05$; multiple testings adjusted), while light pink dots show unchanged genes. Note that the majority of genes have higher transcript abundances in EBs than ESCs, while relatively few transcripts are expressed at higher levels in ESCs.

(B) qRT-PCR validation of transcript abundance arrays. qRT-PCR reactions were carried out using equivalent amounts of RNA from the unfractionated samples of ESCs and EBs. The data were normalized to spiked-in control luciferase RNA. The microarray data showed significant correlation with the qRT-PCR results.

(C) Graphic representation of differential translation. The vertical axis represents the ratio of translational efficiency (i.e., percent polysome associated) for individual transcripts in EBs versus ESCs. The horizontal axis is the average expression level ([EB + ESC] / 2) for each transcript. Orange dots indicate transcripts with significantly increased or decreased translational efficiency in EBs/ESCs, while light orange dots indicate unchanged transcripts (*$p < 0.05$; multiple testings adjusted). Note that the vast majority of transcripts show increased translational efficiency, while none show a decreased efficiency.

(D) qRT-PCR validation of translation state array results. qRT-PCR reactions were carried out using equivalent amounts of polysome-fractionated RNA from the ESCs and EBs and were expressed as a ratio of translational efficiency (i.e., percent polysome associated). Data were normalized to spiked-in control luciferase RNA. The microarray-based measurements of translation state show a significant correlation with qRT-PCR analysis.

(E) Combined analysis of transcriptional and translational regulation during ESC differentiation. The vertical axis shows the EB/ESC translational efficiency ratio, while the horizontal axis shows the EB/ESC transcript abundance ratio. All transcripts with average log intensity >6 are included, and each point on the array represents an individual transcript. Light blue spots show transcripts with statistically significant changes in both abundance and translational efficiency. Pink spots show genes with significant transcript abundance changes but no change in translation state. Orange spots show genes with significant translational efficiency changes but no change in overall abundance. Dark blue spots show genes with no significant changes in either translation state or abundance.

transcript abundance, it is well translated in undifferentiated ESCs and translationally repressed in EBs. A control transcript, β-actin, remained associated with large polysomes in both ESCs and EBs (Figure 4A).

Protein Abundance Follows Predictions from TSAA Analysis

Several candidate gene products were analyzed by immunoblotting, and expected changes in protein levels were observed (Figure 5A). The protein product of DAZL, a gene showing both increased transcript level and polysome association, was significantly increased in differentiating EBs. ATF5 and DCC showed no change in transcript levels but significantly increased polysome association with differentiation. As predicted, both of these proteins were increased in the day 5 EBs compared to ESCs (Figure 5A). Finally, Wnt1 showed no change in transcript level but showed decreased polysome association in EBs. Western blotting showed a significant decrease in protein expression in EBs (Figure 5A). Time-course experiments revealed that DAZL upregulation and Wnt1 downregulation were detectable within

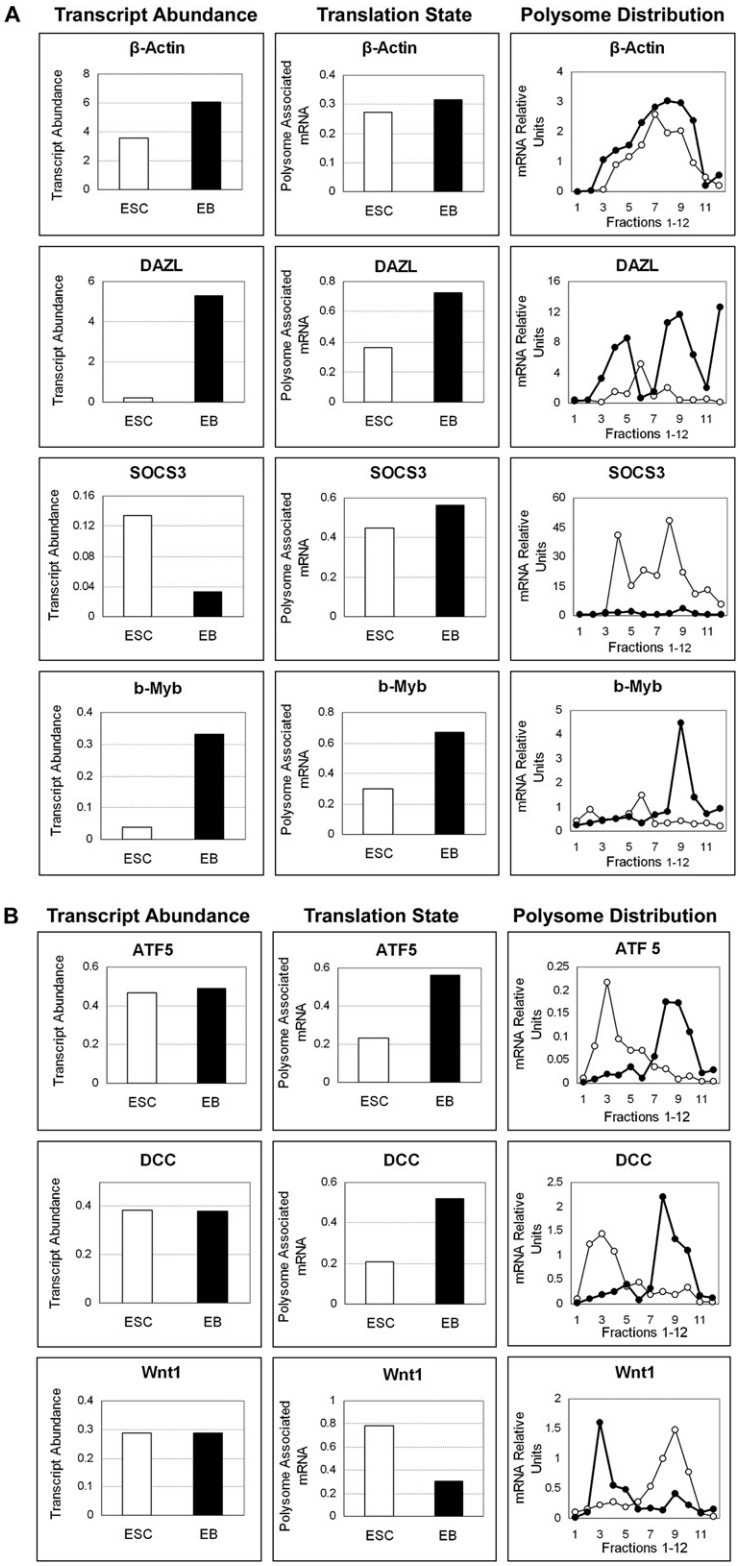

Figure 4. High-Resolution Polysome Prolifes Confirm Differential Regulation of Individual Transcripts

(A and B) Regulation of individual transcripts during differentiation. qRT-PCR validations of transcript abundance and translation state for specific genes in ESCs and EBs in column 1 and column 2, respectively. Clear bars represent qRT-PCR data in ESCs; solid bars represent qRT-PCR data in EBs. (Column 3) The 12 fraction polysomal RNA was subjected to high-resolution qRT-PCR using equivalent amounts of RNA for both EBs and ESCs. Control luciferase RNA normalized signal intensities are plotted on the y axis. Shown are typical profiles of genes differentially expressed. qRT-PCR values display differential distribution of polysomal mRNA. The thin lines with open circles represent ESCs, and the thick lines with closed circles represent EBs. In all cases, high-resolution polysome profiling confirmed results based on analysis of pooled fractions.

24 hr, while ATF5 upregulation was not detected until 48 hr and increases in DCC were not seen until 72 hr (Figure 5B). The different time profiles for these proteins suggest that expression is controlled by several regulators downstream of LIF (Figure 5B). Thus, TSAA provided insights into potential changes in the cellular proteome that could not have been obtained through conventional analysis of mRNA abundance.

Hierarchical Translational Control during Differentiation

As an initial step toward understanding the regulatory mechanisms involved, we determined the phosphorylation states of two molecules that are key in the control of translation initiation. Eukaryotic initiation factor 4E-binding protein (4EBP1) normally inhibits protein translation through sequestration of eIF-4E (Gebauer and Hentze, 2004; Richter and Sonenberg, 2005). When 4EBP1 is phosphorylated by activation of the mTOR pathway, eIF4E is released, resulting in general activation of translation (Parsa and Holland, 2004). We observed that ESC differentiation was accompanied by a marked increase in phospho-4EBP1, suggesting mTOR activation (Figure 5C).

The phosphorylation of the α subunit of eIF-2 is another key site of translational control. In its phosphorylated state, eIF-2α inhibits the guanine nucleotide exchange factor, eIF2B, which in turn inhibits translation initiation (Day and Tuite, 1998; Goss et al., 1984). In contrast to 4EBP1, eIF-2α showed no change in phosphorylation status during ESC differentiation (Figure 5D).

Time-course analysis shows that 4EBP1 phosphorylation is weakly detectable at 12 hr, is readily detectable at 24 hr, and increases further from 1–5 days of differentiation (Figure 5E). To determine whether this is regulated by mTOR, ESCs and EBs were treated with rapamycin, an inhibitor of protein kinase mTOR. Morphologically, rapamycin seemed to slow cell proliferation, resulting in reduced cell density in ESCs and petite EBs (Figure S2). Importantly, no significant cell death was detected. Rapamycin treatment for 3 days results in loss of phosphorylation of 4EBP1, indicating mTOR signaling is activated during ESC differentiation (Figure 5F). We observed an ~17% decrease in the mRNA level and ~25% decrease in ribosome loading of DAZL transcript upon

Table 1. Differential Regulation of Transcripts during ESC Differentiation

Section A

Probe Set ID	Gene Symbol	Transcript Abundance (Fold Change)	Translation State (Fold Change)
1426582	Atf2	2.47	3.70
1424750	Zbtb1	2.47	3.60
1417820	Tor1b	2.47	3.29
1460462	Med18	2.53	3.05
1434884	Mtdh	2.41	2.94
1421122	Cbll1	2.41	2.84
1426722	Slc38a2	2.42	2.80
1428659	Phf7	2.47	2.63
1424820	Ndfip1	2.51	2.60

Section B

Probe Set ID	Gene Symbol	Transcript Abundance (Fold Change)	Translation State (Fold Change)
1428845	Bclaf1	7.11	1.39
1423066	Dnmt3a	6.68	1.04
1429777	Dnajb6	5.93	1.27
1451352	Mta3	5.77	1.09
1418488	Ripk4	5.35	1.37
1419241	Aire	5.31	1.23
1452246	Ostf1	5.20	1.30
1452186	Rbm5	5.09	1.29

Section C

Probe Set ID	Gene Symbol	Transcript Abundance (Fold Change)	Translation State (Fold Change)
1438708	Ywhab	1.07	2.26
1433442	Klhl9	1.13	2.25
1425927	Atf5	1.08	2.20
1420023	Etf1	1.07	2.09
1437226	Mlp	0.98	1.98
1452519	Zfp36	1.06	1.82
1448213	Anxa1	1.06	1.79
1460038	Pou3f1	1.07	1.62
1417028	Trim2	1.05	1.53

Section A, selected genes with altered transcript abundance or translation state showing homodirectional changes. Section B, gene list that displays increased transcript abundance >4-fold but not well translated. Section C, gene list that displays only differential translation state, but no change in transcript level.

treatment with rapamycin in the differentiating EBs (Figure S3), suggesting both transcript levels and translation efficiency contribute to a reduction in protein levels. Further, protein expression of DAZL, but not of ATF5, is markedly downregulated by rapamycin (Figure 5F), suggesting there are mTOR-dependent and -independent pathways for translational regulation.

Although all the downstream targets of mTOR are still not clear, our data suggest that DAZL is one of the targets of mTOR signaling. DAZL, an RNA-binding protein, in turn regulates translation of a subgroup of mRNAs in germ cell differentiation (Collier et al., 2005). This suggested the possibility of a hierarchical pathway for translational regulation during ESC differentiation. To explore this possibility, we knocked down DAZL using siRNA and studied the translation of one of its known targets, guanine-rich sequence factor (GRSF1) (Jiao et al., 2002). GRSF1 is of interest because it is also an mRNA-binding translational regulator. As shown in Figure 5H, GRSF1 mRNA and protein expression are markedly upregulated in differentiated EBs. Delivery of siRNA resulted in an 80% knockdown of DAZL transcript levels and a 60% knockdown of protein, while a scrambled sequence had no effect. In DAZL knockdown cells, an 80% decrease in the protein expression of GRSF1 was observed, but not in control cells transfected with scrambled siRNA (Figure 5H). As expected, GRSF1 mRNA level is not affected (Figure 5G), indicating that DAZL regulates GRSF1 mRNA translation in EBs. β-actin mRNA and protein levels are not significantly affected by DAZL knockdown. These data point to a hierarchy of translational regulation during ESC differentiation involving mTOR, 4EBP1 phosphorylation, DAZL, and GRSF1.

DISCUSSION

ESCs have a remarkable potential to differentiate into all cell types in the adult organism, as well as to self-renew in an undifferentiated state without senescing or becoming neoplastic. Differentiation is accompanied by an increase in cellular complexity, as observed by the development of well-defined endoplasmic reticulum and Golgi bodies, organelles involved in protein synthesis in the EBs. The molecular mechanisms that underlie the transition from undifferentiated to differentiated states remain unclear, however. By an integrated analysis of ribosome loading combined with the conventional transcriptome profiling, we have presented a holistic view of gene expression during the differentiation of ESCs. The use of spiked-in cRNA standards to normalize gene expression, rather than using total signal on the array or housekeeping genes, revealed a previously unrecognized global increase in transcript abundance, paralleled by a coordinate increase in ribosome loading for a majority of genes as ESCs differentiate. This was supported by the observation that ESCs clearly possess a surplus of free ribosomes, which are found as single ribosomes and ribosomal subunits and are recruited into actively translating polysomes during differentiation. It seems, therefore, that the protein synthesis capacity of ESCs is poised to allow rapid elevation of translation rate in response to differentiation signals.

While the mechanism for this global increase in mRNA expression is not known, some insights come from recent studies on transcriptional initiation and elongation in undifferentiated human ESCs (Guenther et al., 2007). These authors found that most genes contained chromatin signatures characteristic of transcriptional initiation (RNA polymerase II [Pol II]), coupled with nucleosomes containing trimethyl lysines 4 and 9 on histone H3, yet were not expressed. This suggests that transcript elongation is rate limiting in the undifferentiated state. A similar mechanism has been described in yeast, where many genes have Pol II positioned for activation upon signals that promote exit of stationary phase (Radonjic et al., 2005). Having potentially important loci "poised" for transcription may facilitate a rapid

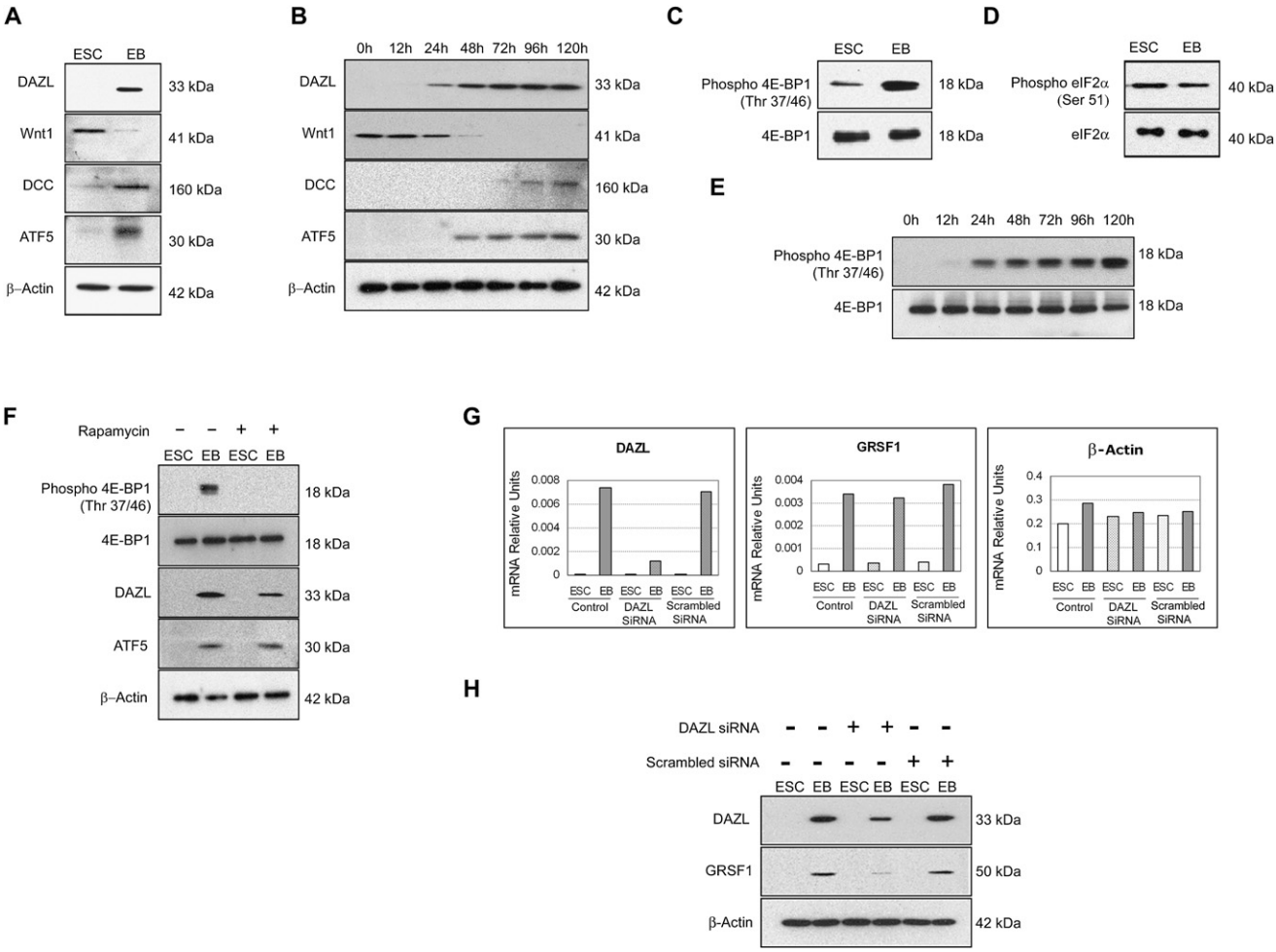

Figure 5. Protein Expression and Mechanistic Analysis of Translational Regulation

(A) Protein expression from translationally controlled genes. Western blot analyses of DAZL, WNT1, ATF5, and DCC expression in ESCs and EBs. Beta-actin expression was analyzed as the loading control. DAZL, ATF5, and DCC show a marked increase in protein expression in EBs, whereas Wnt1 displays decreased expression in EBs.

(B) Time-course analysis. Changes in DAZL and Wnt1 are apparent within 24 hr of LIF withdrawal. Increased ATF5 levels could be seen by 48 hr, whereas increases in DCC were detectable by 72 hr.

(C and D) Phosphorylation state of translation regulators. Western blot analyses of ESCs and EB lysates were performed for phospho-4E-BP1 and phospho-eIF-2α along with their control proteins 4E-BP1 and eIF-2α in the upper and lower panels, respectively. A marked increase in phospho-4E-BP1 was observed in EBs. However, eIF-2α does not show a significant change in phosphorylation status during ESC differentiation.

(E) Time-course analysis of 4EBP1 phosphorylation during ESC differentiation. 4EBP1 phosphorylation was detectable by 12 hr and increased progressively with differentiation.

(F) mTOR signaling and target identification during ESC differentiation. Treatment with rapamycin leads to loss of 4EBP1 phosphorylation. Expression of DAZL, but not ATF5, is markedly downregulated by rapamycin.

(G) Knockdown of DAZL transcript by siRNA. DAZL mRNA is markedly diminished by DAZL siRNA, but not by scrambled siRNA. Transcript levels of the DAZL target, GRSF1, or β-actin are unaffected by DAZL knockdown.

(H) DAZL regulates translation of its target mRNA GRSF1 in differentiated ESCs. In DAZL knockdown cells, GRSF1 protein expression is significantly downregulated, while scrambled siRNA has no effect. β-actin protein levels in DAZL knockdown cells are unchanged versus control.

change of state when signals favor differentiation. As an alternate, nonexclusive mechanism, repression of transcriptional repressors including Klf4, Pax3, Twist2, Strm, and Zfhx1b and the repression of polycomb group (PcG) proteins that occupy the promoter sites of Fox, Gata, Sox, and Tbx genes (Boyer et al., 2006) may potentially facilitate increased transcription in EBs. A third formal possibility is increased transcript stability, although there are currently no data to support this.

We show that ESC differentiation was accompanied by a 2-fold increase in the rate of protein synthesis, resulting in ~30% more steady-state protein per cell. These biochemical indices correlated well with cellular ultrastructure, which showed increased cytoplasmic volume and the development of organelles associated with protein synthesis. Interestingly, although ESCs had a number of free ribosomes, these were present predominantly as monosomes or subunits, indicating

untapped translational potential. In contrast, cells in EBs showed an ~60% increase in their polysome fraction of the cytoplasmic lysate. When ribosomal loading of individual transcripts was examined by TSAA, we observed a global increase in polysome association, suggesting enhanced translational efficiency. We observed that 78% of the transcripts expressed in both ESCs and EBs showed statistically significant increases in ribosome loading. Taken together, these data indicate that protein production from the majority of genes is limited in ESCs by both transcript availability and rate of translation initiation.

Global regulation of initiation involves modulation of canonical initiation factor activities. Two well-known interactions regulated by switches in phosphorylation states control global translation initiation. These include 4EBP1, which competes with eIF4G to bind the cap-binding protein eIF4E, and eIF2α, a component of the ternary complex. In the differentiated progeny, no significant modulation of phosphorylation state of eIF2α was observed. However, hyperphosphorylation of 4EBP1 observed in EBs may prevent sequestration of eIF4E by 4EBP1, leading to increased translation. Rapamycin prevented 4EBP1 phosphorylation in EBs, indicating that the mTOR pathway is an important component of the anabolic switch observed in ESC differentiation.

LIF activation of the PI3K/Akt pathway is known to be essential for survival and maintenance of pluripotency in ESCs (Gross et al., 2005; Watanabe et al., 2006). However, in ESCs, the downstream effectors of Akt in LIF signaling are not well characterized. Conventionally, Akt signaling occurs through mTOR. Our data show that in the presence of LIF, phosphorylation of 4EBP1 occurs at a very basal level, leading to sequestration of eIF4E and parsimonious translation. This suggests that, in the ESCs, either there is a repressor of 4EBP1 phosphorylation or an alternative pathway that dephosphorylates 4EBP1. Nevertheless, proliferation of ESCs was slowed by rapamycin treatment, suggesting that low-level signaling through mTOR is occurring in the undifferentiated state and is physiologically significant.

Although the translation of most capped mRNAs can be regulated through mTOR, some mRNAs are more sensitive to rapamycin than others, suggesting mTOR-dependent and -independent mechanisms. DAZL, an RNA-binding protein that displays strong upregulation both in transcript abundance and translation state in differentiated EBs, was found to be rapamycin sensitive, whereas the transcription factor ATF5 was not affected. Structural features and regulatory sequences within the mRNA modulate its translation fate (Gray and Wickens, 1998). ATF5 translation could be regulated by an alternative mechanism, such as by the uORFs in its 5′UTR (Watatani et al., 2007) or by miRNAs.

Modifications of 5′ m7 GpppX cap and a 3′ poly(A) tail found in most eukaryotic mRNAs synergistically enhance the translational efficiency of the mRNA (Gebauer and Hentze, 2004). Further, interaction of these factors facilitates the speed and accuracy of translation initiation and also provides an opportunity for regulation. DAZL activates translationally silent mRNAs through the recruitment of polyadenylate-binding proteins (PABPs) and further stimulates translation by enhancing the rate of initiation, by increasing 80S formation (Collier et al., 2005; Yen, 2004). Several mDAZL target mRNAs have been identified, containing a 26 nucleotide region in the 3′UTR, necessary and sufficient to bind mDAZL (Jiao et al., 2002). We showed that, in differentiating ESCs, DAZL knockdown by siRNA leads to decreased translation of its specific target mRNAs like GRSF1.

Interestingly, GRSF1 was identified as a target of the Wnt/β-catenin pathway that mediated important effects on mesoderm formation, brain development, and posterior axis elongation (Lickert et al., 2005). From our microarray data we know that Wnt3a and Wnt8a are transcriptionally and translationally upregulated in EBs. These factors could be responsible for inducing GRSF1 transcription, while DAZL is required for its translation. GRSF1 is also known to regulate selective translation of eukaryotic mRNAs by binding to specific 5′UTR GRSF1-binding sites (Kash et al., 2002). Thus, our data implicate a hierarchy of translation controls that involves global translation regulators like mTOR and phospho-4EBP1, followed by target mRNA-binding proteins like DAZL, which in turn modulate other translational regulators like GRSF1. Such translational regulatory circuits control selective protein expression, and potentially direct differentiation of ESCs to specific cell lineages (Figure 6).

Transcriptional regulation is crucial for certain phases of growth and development; however, during eukaryotic embryogenesis the earliest phases of development rely on the selective translation of transcript reserves (de Moor and Richter, 2001). In our study we found a few genes including Wnt1, ATF5, and DCC regulated exclusively at the translational level. ATF5, a transcription factor important in differentiation, proliferation, and survival, is highly expressed in neural progenitor cells and in certain tumors, including glioblastomas (Monaco et al., 2007). ATF5 is under stringent translational repression in ESCs, and its expression in EBs may be potentially important for differentiation of neural progenitor cells. DCC has been proposed to function as a metastasis suppressor gene regulating both proinvasive and survival pathways in a cumulative manner (Rodrigues et al., 2007).

Interestingly, very few transcripts showed a decrease in their translation state during EB formation, suggesting that transcriptional repression is a major mechanism downregulating protein expression, during differentiation. A notable exception was Wnt1, which showed no significant change in transcript level during differentiation but displayed differential translation. The Wnt/β-catenin pathway is important for maintaining pluripotency (Miyabayashi et al., 2007), and as embryogenesis proceeds this pathway regulates key events such as mesoderm formation and activation or repression of terminal cell fates (Naito et al., 2006). We speculate that sequestration of Wnt1 transcripts in nontranslated fractions of differentiating cells is a means to repress this pathway, while retaining the ability to activate it rapidly under appropriate cues.

Our work has clearly shown that ESC differentiation is accompanied by marked increases in translational efficiency. The differentiated EBs have polysome profiles that are comparable to other highly metabolically active cells, e.g., HeLa cells (Nilsen et al., 1982) or activated T cells (Garcia-Sanz et al., 1998; Grolleau et al., 2002), whereas the undifferentiated ESCs have polysome profiles that are comparable to quiescent T cells (Garcia-Sanz et al., 1998; Grolleau et al., 2002). In contrast to quiescent T cells, however, the ESCs are actively proliferating, with cell-cycle times of ~17 hr. This points to the relative simplicity of the ESC proteome compared to T cells or HeLa cells, both of which require greater protein synthesis rates to maintain comparable cell division rates. What justifies the metabolic cost of

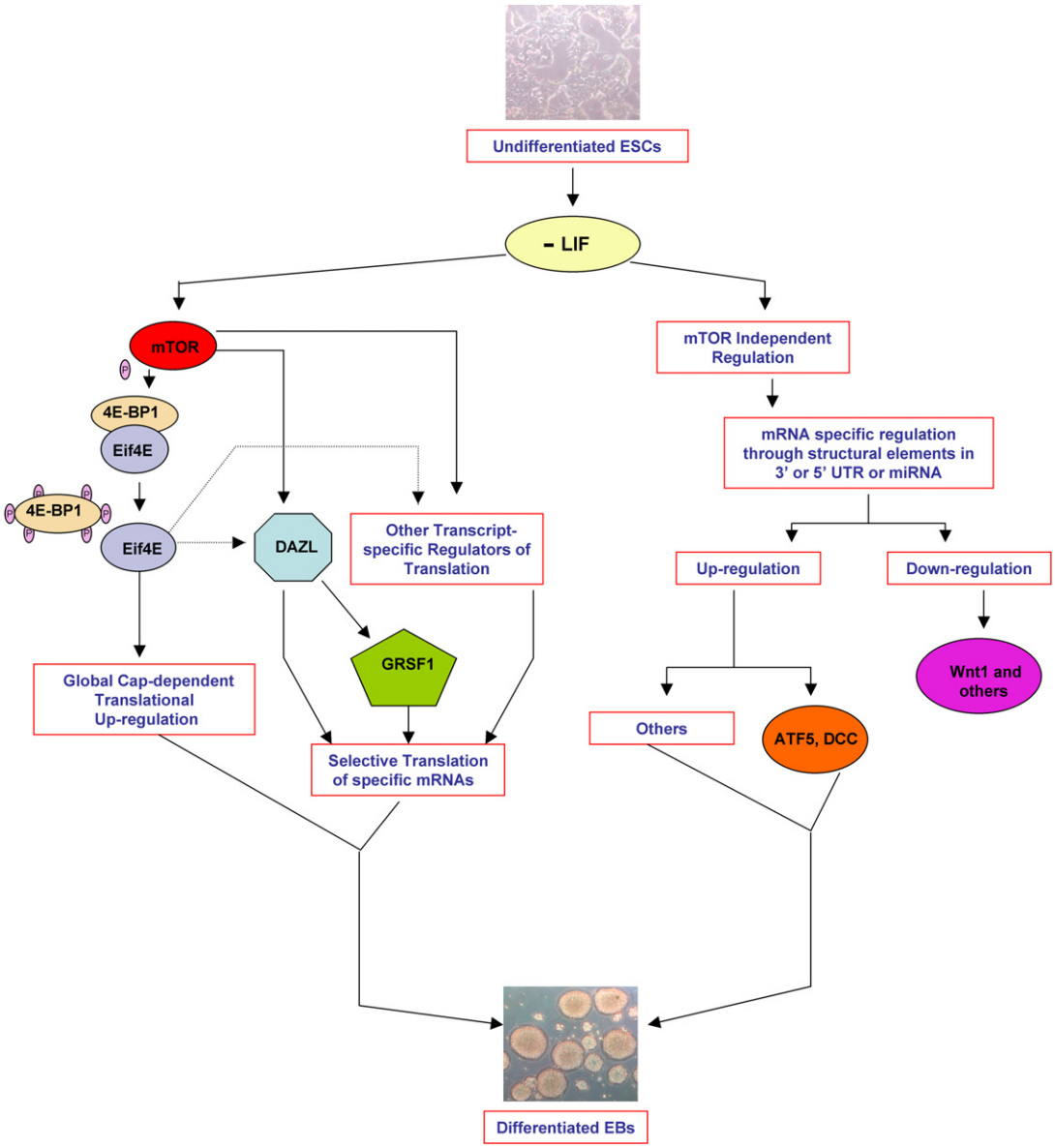

Figure 6. Schematic Representation of Translational Regulation during Embryonic Stem Cell Differentiation

During ESC self-renewal, low basal activity of mTOR leads to parsimonious translation. During ESC differentiation, a hierarchy of translational regulators controls differentiation. LIF withdrawal strongly activates the mTOR pathway, leading to release of eIF4E and a global increase in translation of Cap-dependent transcripts. mTOR activation also leads to sequential translation of the mRNA-binding proteins DAZL and GRSF1, which in turn can facilitate selective translation of downstream targets. mTOR-independent pathway leads to translation of other genes, including ATF5 and DCC.

maintaining unassembled ribosomal subunits and duplicating them with each round of cell division? We speculate that availability of these subunits facilitates rapid changes in mRNA translation when appropriate cues to differentiate are received. From early embryonic development to cell differentiation, translational control is used to fine-tune protein levels. Dysregulation of any of the translation regulators could adversely affect translation of various genes during ESC differentiation. We propose that parsimonious translation prior to differentiation, along with a hierarchy of translational regulators during differentiation, provides quality controls that ensure translation only of appropriate transcripts. As a deeper understanding of translational control emerges, it may prove useful in directing the differentiation of ESCs to desired cell types.

EXPERIMENTAL PROCEDURES

Cell Culture

Mouse ESCs (line R1) were cultured in gelatin-coated tissue culture dishes in the presence of LIF to maintain them in an undifferentiated state. For genome-wide experiments, cells were cultured in DMEM supplemented with 15% fetal bovine serum (FBS) (Hyclone, Logan, UT), 450 μM monothioglycerol (MTG) (Sigma-Aldrich, St. Louis), and 1000 U/ml LIF (Esgro, Temecula, CA). The medium was supplemented with 1 μg/ml penicillin/streptomycin (Sigma-Aldrich). Cells were collected when they were 40%–50% confluent. Further, ESCs were

cultured in the absence of LIF on low-attachment plates for 5 days to form EBs and collected for further experimental analysis. Three biological replicates of ESCs and EB cultures were used for polysome fractionation and unfractionated RNA extraction.

Transmission Electron Microscopy

Cells were fixed in 10 ml fixative (2.2% glutaraldehyde in 100 mM $NaPO_4$ [pH 7.4]) for 2 hr. Later, they were postfixed in 1% osmium tetroxide, stained en bloc with 0.5% uranyl acetate in water, dehydrated in a graded ethanol series, embedded, and thin sectioned. Sections were stained with 2% uranyl acetate in methanol for 20 min, followed by lead citrate for 5 min, and viewed on a 2000FX transmission electron microscope. Images were processed using Photoshop (Adobe, San Jose, CA). To calculate cytoplasm and nuclear areas, images obtained at 4000× magnification were overlaid with a 208 crosspoint grid in Photoshop. Points over nuclear and cytoplasmic profiles were collected. For each image, a nuclear ratio and a cytoplasmic ratio was calculated as the number of points for a given compartment divided by the sum total of points. Mean nuclear ratio and mean cytoplasmic ratio were calculated as the grand total of the ratios divided by the number of analyzed areas.

Polysome Fractionation

For polysome fractionation, ~1×10^7 cells were incubated with 150 μg/ml of cycloheximide (Sigma-Aldrich) for 15 min to arrest ribosome movement on mRNAs before harvesting the cells. The harvested cells were lysed using MPER modified by the addition of 10 mM KCl, 15 mM $MgCl_2$, 40 U/μl of RNasin (Fermentas), and 1 mM DTT. The cell pellet was suspended in 1 ml of the lysis buffer, homogenized with 10 strokes in a glass homogenizer, and subjected to centrifugation for 30 min at 14,000 rpm to obtain clarified lysate. Absorbance at 260 nm was measured using an aliquot of the supernatant collected. For polysome fractionation, 30 optical density (OD) A_{260} units of the lysate in 1 ml lysis buffer was loaded onto 11 ml linear 7%–47% sucrose gradients in 50 mM Tris-HCl (pH 7.5), 0.8 M KCl, 15 mM $MgCl_2$, 0.5 mg/ml heparin, and 100 μg/ml cycloheximide and centrifuged at 130,000 × g in an SW40-Ti swinging bucket rotor (Beckman) for 1.5 hr at 4°C.

Twelve fractions were collected from the top of the gradients into cold microfuge tubes and immediately placed on ice. Polysome profiles were monitored at 254 nm using an ISCO UA-6 UV detector. The absorbance trace established the positions of mRNAs loaded with 1–8 ribosomes. The positions of higher oligomers were estimated by extrapolation of a curve fit to these points. Each fraction was adjusted to 0.5% SDS, and the 12 fractions were combined to form four pools. Fractions 1–4, 5–7, 8–11, and 12 were combined as pools 1, 2, 3, and 4, respectively (Figure 2A). One milliliter of each pool was used for further analysis, and the data were back corrected for the different pool volumes as described below. In parallel, total RNA was also isolated from unfractionated lysates for transcriptional analysis.

RNA Isolation from Polysome Fractions

To each 1 ml fraction pool, equivalent amounts of synthetic Poly(A)$^+$ luciferase RNA (10 ng/ml) along with bacterial spike-in control RNA were added. Synthetic luciferase RNA serves as a control for the efficiency of RNA isolation and qRT-PCR analysis. The bacterial spike-in RNA was purchased from Affymetrix and has different concentrations of each of the four exogenous, premixed, polyadenylated prokaryotic RNA controls. The prokaryotic genes used as spike-in controls have limited crosshybridization with mammalian sequences but have target sequences on the Affymetrix arrays, and hence serve as controls for both mRNA isolation and hybridization efficiency. RNA was precipitated at −70°C with 2.5 volumes 100% ethanol and purified using QIAGEN RNeasy midi-columns. Eluted RNA was precipitated with 1/10 volume of 10 mM LiCl and resuspended in 25 μl of RNase-free H_2O. The quality of RNA was determined using an Agilent Bioanalyzer and quantitated by absorbance at 260 nm. Isolated RNA was then stored at −70°C. For total unfractionated RNA, after addition of spike-in controls to 1/12 volume of 30 OD A_{260} units in 1 ml of lysis buffer, samples were subjected to ethanol precipitation. Total RNA was isolated, analyzed, and stored the same way as the RNA from polysomal fractions.

Microarray Hybridization

Probes were synthesized by standard Affymetrix procedure, using RNA isolated from unfractionated lysates and fractionated pooled lysates. Biotin-labeled cRNA was purified using RNeasy minikit, fragmented, and hybridized to the Affymetrix 430_2 mouse expression arrays. For probe synthesis, cRNA was synthesized from three biological replicates using standard procedures. After empirical testing, 2.5 μg of polysomal RNA was used in each labeling reaction for all four polysomal pools from both ESC and EB samples. For consistency, same labeling conditions were used for unfractionated RNA samples.

Transcript Abundance Analysis

Unfractionated total RNA samples from ESCs and EBs (1 ml out of 12 ml total volume, corresponding to 30 OD A_{260} units) were used for overall transcript abundance analysis. Three biological replicates of both the ESC and EB samples were prepared. The hybridization intensities were normalized and transformed to log(2) intensity values. External spike-in normalization was performed as described in the Supplemental Experimental Procedures. Identification of differentially expressed genes was performed using the limma analysis package (Smyth, 2004) of the open-source Bioconductor project (http://www.bioconductor.org). Modified probe-set expression intensity data were imported into limma. Limma was then used to fit a linear model to the data. Limma uses an empirical bayes method to moderate the standard errors of the estimated log-fold changes. For all experimental comparisons, P values were calculated with corrections for multiple testing implemented through the "fdr" function of limma that uses the method of Benjamini and Hochberg (Hochberg and Benjamini, 1990). Genes with multiple testing adjusted P value of <.05 were flagged as differentially expressed. Significance analysis of microarrays (SAM) (Tusher et al., 2001) algorithm implemented in the open source MEV program (Saeed et al., 2003) was used to verify the differentially expressed genes. Here a false discovery rate of $p < .05$ was used.

Translation State Analysis

Differentially translated genes were identified using the data generated from the four pools following a modification of the procedure employed for the unfractionated RNA analysis. This analysis is based upon the fact that the majority of messages bound to multiple ribosomes are in pool 3, while pools 1 and 2 contain mRNAs bound to no ribosomes and, at most, 1–3 ribosomes, respectively. Pool 4 contains mRNA bound to very high molecular weight complexes (which likely contain mRNP particles and other currently undefined elements). Consequently, the percentage of a transcript that resides in pool 3 is a measure of translational efficiency. For each replicate ESC and EB sample, we calculated the fraction of normalized log(2) transformed message intensity in pool 3 divided by the total message intensity (pool 3 / [pool 1+2+3+4]). To correct for different initial volumes of the four pools, we weighted the contribution of each pool based on its starting volume according to the equation (pool 3 intensity × 4) / ([pool 1 intensity × 4] + [pool 2 intensity × 3] + [pool 3 intensity × 4] + [pool 4 intensity × 1]) for each replicate. A comparison of this weighted "recombination" of the fractionated pools versus the unfractionated mRNA indicated a good linear correlation (see Results). A limma analysis (multiple testings adjusted $p < .05$) was performed as described for the unfractionated RNA analysis to identify differentially translated genes that show statistically significant changes in percentage of transcripts in pool 3.

Inhibitor and Knockdown Studies

To block mTOR signaling, cells were treated with rapamycin (Calbiochem) at a concentration of 20 ng/ml. Cells were collected for western blot analysis after 3 days of treatment. To knock down DAZL, predesigned siRNA from Ambion was used along with Silencer siRNA transfection II kit and siPORT NeoFX transfection agent, following the manufacturer's protocol. Three-day-old cells were collected for qRT-PCR and western blot analysis.

Quantitative RT-PCR

Specific transcripts were quantified using premade or custom-made Taqman gene expression assays from Applied Biosystems, Inc. (ABI). Custom primers and probes were designed using file builder software from ABI. Triplicate samples and negative controls were included to ensure accuracy. qRT-PCR data were normalized with synthetic luciferase RNA added as a spike-in control

before RNA isolation. Fraction pool ratios were calculated for the qRT-PCR data to allow comparison with microarray data.

Western Blotting

ESCs and EBs collected were washed with Dulbecco's modified PBS. The cells were then lysed on ice by the addition of MPER supplemented with 1% Protease Inhibitor Cocktail (Roche). The lysate was homogenized by repeated passage through a 26 gauge needle. For immunoblot analysis, cell lysates were resolved by SDS-PAGE using 12% polyacrylamide gels and transferred to Immobilon-P (Millipore) by a semidry transfer protocol. The blot was probed with anti-DAZL (1:5000) (Abcam), anti-GRSF1 (1:500) (Novus Biological), anti-ATF5 (1:2000) (Abcam), anti-DCC (1: 2000), anti-Wnt1 (1:2000), or anti-β-actin (1:7000) (Abcam) antibody and detected with goat anti-mouse, rabbit anti-goat, or goat anti-rabbit IgG labeled with horseradish peroxidase (Abcam, Cambridge, MA). The membrane was incubated with chemiluminescent substrate (SuperSignal West Dura; Pierce) for 5 min at room temperature and exposed to X-ray film (Kodak).

ACCESSION NUMBERS

Microarray data deposited in GEO have the accession number GSE9563.

SUPPLEMENTAL DATA

Supplemental Data include three figures and Supplemental Experimental Procedures and can be found with this article online at http://www.cellstemcell.com/cgi/content/full/2/5/448/DC1/.

ACKNOWLEDGMENTS

The authors are indebted to Mr. James Fugate, Mr. Jason M. Daza, Ms. Brittany Hopkins, and Ms. Veronica Muskheli for technical assistance. We thank Dr. Roger Bumgarner, Ms. Becky Drees, and Mr. Robert W. Hall at the University of Washington Center for Expression Arrays for assistance with microarray analysis. The array work was subsidized through NIH grant HL072370. We thank Dr. Larry Ruzzo for helpful discussions. This work was supported by NIH grants HL61553, HL64387, HL84642, and GM69983 (to C.E.M.); HL3174 (to S.M.S. and C.E.M.); CA89807 (to D.R.M.); and Rosetta/Merck postdoctoral fellowship (to P.S.).

Received: October 18, 2007
Revised: February 2, 2008
Accepted: March 19, 2008
Published: May 7, 2008

REFERENCES

Ali, N.N., Edgar, A.J., Samadikuchaksaraei, A., Timson, C.M., Romanska, H.M., Polak, J.M., and Bishop, A.E. (2002). Derivation of type II alveolar epithelial cells from murine embryonic stem cells. Tissue Eng. *8*, 541–550.

Angelastro, J.M., Ignatova, T.N., Kukekov, V.G., Steindler, D.A., Stengren, G.B., Mendelsohn, C., and Greene, L.A. (2003). Regulated expression of ATF5 is required for the progression of neural progenitor cells to neurons. J. Neurosci. *23*, 4590–4600.

Angelastro, J.M., Mason, J.L., Ignatova, T.N., Kukekov, V.G., Stengren, G.B., Goldman, J.E., and Greene, L.A. (2005). Downregulation of activating transcription factor 5 is required for differentiation of neural progenitor cells into astrocytes. J. Neurosci. *25*, 3889–3899.

Arava, Y. (2003). Isolation of polysomal RNA for microarray analysis. Methods Mol. Biol. *224*, 79–87.

Arava, Y., Wang, Y., Storey, J.D., Liu, C.L., Brown, P.O., and Herschlag, D. (2003). Genome-wide analysis of mRNA translation profiles in Saccharomyces cerevisiae. Proc. Natl. Acad. Sci. USA *100*, 3889–3894.

Bader, A., Al-Dubai, H., and Weitzer, G. (2000). Leukemia inhibitory factor modulates cardiogenesis in embryoid bodies in opposite fashions. Circ. Res. *86*, 787–794.

Bain, G., Kitchens, D., Yao, M., Huettner, J.E., and Gottlieb, D.I. (1995). Embryonic stem cells express neuronal properties in vitro. Dev. Biol. *168*, 342–357.

Beissbarth, T., and Speed, T.P. (2004). GOstat: find statistically overrepresented Gene Ontologies within a group of genes. Bioinformatics *20*, 1464–1465.

Boyer, L.A., Plath, K., Zeitlinger, J., Brambrink, T., Medeiros, L.A., Lee, T.I., Levine, S.S., Wernig, M., Tajonar, A., Ray, M.K., et al. (2006). Polycomb complexes repress developmental regulators in murine embryonic stem cells. Nature *441*, 349–353.

Cai, L., Ye, Z., Zhou, B.Y., Mali, P., Zhou, C., and Cheng, L. (2007). Promoting human embryonic stem cell renewal or differentiation by modulating Wnt signal and culture conditions. Cell Res. *17*, 62–72.

Chinzei, R., Tanaka, Y., Shimizu-Saito, K., Hara, Y., Kakinuma, S., Watanabe, M., Teramoto, K., Arii, S., Takase, K., Sato, C., et al. (2002). Embryoid-body cells derived from a mouse embryonic stem cell line show differentiation into functional hepatocytes. Hepatology *36*, 22–29.

Collier, B., Gorgoni, B., Loveridge, C., Cooke, H.J., and Gray, N.K. (2005). The DAZL family proteins are PABP-binding proteins that regulate translation in germ cells. EMBO J. *24*, 2656–2666.

Day, D.A., and Tuite, M.F. (1998). Post-transcriptional gene regulatory mechanisms in eukaryotes: an overview. J. Endocrinol. *157*, 361–371.

de Moor, C.H., and Richter, J.D. (2001). Translational control in vertebrate development. Int. Rev. Cytol. *203*, 567–608.

Dvash, T., Mayshar, Y., Darr, H., McElhaney, M., Barker, D., Yanuka, O., Kotkow, K.J., Rubin, L.L., Benvenisty, N., and Eiges, R. (2004). Temporal gene expression during differentiation of human embryonic stem cells and embryoid bodies. Hum. Reprod. *19*, 2875–2883.

Forrai, A., Boyle, K., Hart, A.H., Hartley, L., Rakar, S., Willson, T.A., Simpson, K.M., Roberts, A.W., Alexander, W.S., Voss, A.K., and Robb, L. (2006). Absence of suppressor of cytokine signalling 3 reduces self-renewal and promotes differentiation in murine embryonic stem cells. Stem Cells *24*, 604–614.

Garcia-Sanz, J.A., Mikulits, W., Livingstone, A., Lefkovits, I., and Mullner, E.W. (1998). Translational control: a general mechanism for gene regulation during T cell activation. FASEB J. *12*, 299–306.

Gebauer, F., and Hentze, M.W. (2004). Molecular mechanisms of translational control. Nat. Rev. Mol. Cell Biol. *5*, 827–835.

Goss, D.J., Parkhurst, L.J., Mehta, H.B., Woodley, C.L., and Wahba, A.J. (1984). Studies on the role of eukaryotic nucleotide exchange factor in polypeptide chain initiation. J. Biol. Chem. *259*, 7374–7377.

Gray, N.K., and Wickens, M. (1998). Control of translation initiation in animals. Annu. Rev. Cell Dev. Biol. *14*, 399–458.

Grolleau, A., Bowman, J., Pradet-Balade, B., Puravs, E., Hanash, S., Garcia-Sanz, J.A., and Beretta, L. (2002). Global and specific translational control by rapamycin in T cells uncovered by microarrays and proteomics. J. Biol. Chem. *277*, 22175–22184.

Gross, V.S., Hess, M., and Cooper, G.M. (2005). Mouse embryonic stem cells and preimplantation embryos require signaling through the phosphatidylinositol 3-kinase pathway to suppress apoptosis. Mol. Reprod. Dev. *70*, 324–332.

Guenther, M.G., Levine, S.S., Boyer, L.A., Jaenisch, R., and Young, R.A. (2007). A chromatin landmark and transcription initiation at most promoters in human cells. Cell *130*, 77–88.

Gunji, W., Kai, T., Sameshima, E., Iizuka, N., Katagi, H., Utsugi, T., Fujimori, F., and Murakami, Y. (2004). Global analysis of the expression patterns of transcriptional regulatory factors in formation of embryoid bodies using sensitive oligonucleotide microarray systems. Biochem. Biophys. Res. Commun. *325*, 265–275.

Hochberg, Y., and Benjamini, Y. (1990). More powerful procedures for multiple significance testing. Stat. Med. *9*, 811–818.

Jiao, X., Trifillis, P., and Kiledjian, M. (2002). Identification of target messenger RNA substrates for the murine deleted in azoospermia-like RNA-binding protein. Biol. Reprod. *66*, 475–485.

Joaquin, M., and Watson, R.J. (2003). Cell cycle regulation by the B-Myb transcription factor. Cell. Mol. Life Sci. *60*, 2389–2401.

Kash, J.C., Cunningham, D.M., Smit, M.W., Park, Y., Fritz, D., Wilusz, J., and Katze, M.G. (2002). Selective translation of eukaryotic mRNAs: functional molecular analysis of GRSF-1, a positive regulator of influenza virus protein synthesis. J. Virol. *76*, 10417–10426.

Katoh, M., and Katoh, M. (2007). WNT signaling pathway and stem cell signaling network. Clin. Cancer Res. *13*, 4042–4045.

Lickert, H., Cox, B., Wehrle, C., Taketo, M.M., Kemler, R., and Rossant, J. (2005). Dissecting Wnt/beta-catenin signaling during gastrulation using RNA interference in mouse embryos. Development *132*, 2599–2609.

Llambi, F., Causeret, F., Bloch-Gallego, E., and Mehlen, P. (2001). Netrin-1 acts as a survival factor via its receptors UNC5H and DCC. EMBO J. *20*, 2715–2722.

MacKay, V.L., Li, X., Flory, M.R., Turcott, E., Law, G.L., Serikawa, K.A., Xu, X.L., Lee, H., Goodlett, D.R., Aebersold, R., et al. (2004). Gene expression analyzed by high-resolution state array analysis and quantitative proteomics: response of yeast to mating pheromone. Mol. Cell. Proteomics *3*, 478–489.

Miyabayashi, T., Teo, J.L., Yamamoto, M., McMillan, M., Nguyen, C., and Kahn, M. (2007). Wnt/beta-catenin/CBP signaling maintains long-term murine embryonic stem cell pluripotency. Proc. Natl. Acad. Sci. USA *104*, 5668–5673.

Monaco, S.E., Angelastro, J.M., Szabolcs, M., and Greene, L.A. (2007). The transcription factor ATF5 is widely expressed in carcinomas, and interference with its function selectively kills neoplastic, but not nontransformed, breast cell lines. Int. J. Cancer *120*, 1883–1890.

Naito, A.T., Shiojima, I., Akazawa, H., Hidaka, K., Morisaki, T., Kikuchi, A., and Komuro, I. (2006). Developmental stage-specific biphasic roles of Wnt/beta-catenin signaling in cardiomyogenesis and hematopoiesis. Proc. Natl. Acad. Sci. USA *103*, 19812–19817.

Nilsen, T.W., Maroney, P.A., and Baglioni, C. (1982). Inhibition of protein synthesis in reovirus-infected HeLa cells with elevated levels of interferon-induced protein kinase activity. J. Biol. Chem. *257*, 14593–14596.

Parsa, A.T., and Holland, E.C. (2004). Cooperative translational control of gene expression by Ras and Akt in cancer. Trends Mol. Med. *10*, 607–613.

Potireddy, S., Vassena, R., Patel, B.G., and Latham, K.E. (2006). Analysis of polysomal mRNA populations of mouse oocytes and zygotes: dynamic changes in maternal mRNA utilization and function. Dev. Biol. *298*, 155–166.

Pradet-Balade, B., Boulme, F., Beug, H., Mullner, E.W., and Garcia-Sanz, J.A. (2001). Translation control: bridging the gap between genomics and proteomics? Trends Biochem. Sci. *26*, 225–229.

Preiss, T., Baron-Benhamou, J., Ansorge, W., and Hentze, M.W. (2003). Homodirectional changes in transcriptome composition and mRNA translation induced by rapamycin and heat shock. Nat. Struct. Biol. *10*, 1039–1047.

Pritsker, M., Ford, N.R., Jenq, H.T., and Lemischka, I.R. (2006). Genome-wide gain-of-function genetic screen identifies functionally active genes in mouse embryonic stem cells. Proc. Natl. Acad. Sci. USA *103*, 6946–6951.

Radonjic, M., Andrau, J.C., Lijnzaad, P., Kemmeren, P., Kockelkorn, T.T., van Leenen, D., van Berkum, N.L., and Holstege, F.C. (2005). Genome-wide analyses reveal RNA polymerase II located upstream of genes poised for rapid response upon S. cerevisiae stationary phase exit. Mol. Cell *18*, 171–183.

Ramalho-Santos, M., Yoon, S., Matsuzaki, Y., Mulligan, R.C., and Melton, D.A. (2002). "Stemness": transcriptional profiling of embryonic and adult stem cells. Science *298*, 597–600.

Richter, J.D., and Sonenberg, N. (2005). Regulation of cap-dependent translation by eIF4E inhibitory proteins. Nature *433*, 477–480.

Rodrigues, S., De Wever, O., Bruyneel, E., Rooney, R.J., and Gespach, C. (2007). Opposing roles of netrin-1 and the dependence receptor DCC in cancer cell invasion, tumor growth and metastasis. Oncogene *26*, 5615–5625.

Saeed, A.I., Sharov, V., White, J., Li, J., Liang, W., Bhagabati, N., Braisted, J., Klapa, M., Currier, T., Thiagarajan, M., et al. (2003). TM4: a free, open-source system for microarray data management and analysis. Biotechniques *34*, 374–378.

Serikawa, K.A., Xu, X.L., MacKay, V.L., Law, G.L., Zong, Q., Zhao, L.P., Bumgarner, R., and Morris, D.R. (2003). The transcriptome and its translation during recovery from cell cycle arrest in Saccharomyces cerevisiae. Mol. Cell. Proteomics *2*, 191–204.

Smith, A.G., Heath, J.K., Donaldson, D.D., Wong, G.G., Moreau, J., Stahl, M., and Rogers, D. (1988). Inhibition of pluripotential embryonic stem cell differentiation by purified polypeptides. Nature *336*, 688–690.

Smyth, G.K. (2004). Linear models and empirical bayes methods for assessing differential expression in microarray experiments. Stat. Appl. Genet. Mol. Biol. *3*, Article3.

Tusher, V.G., Tibshirani, R., and Chu, G. (2001). Significance analysis of microarrays applied to the ionizing radiation response. Proc. Natl. Acad. Sci. USA *98*, 5116–5121.

Watanabe, S., Umehara, H., Murayama, K., Okabe, M., Kimura, T., and Nakano, T. (2006). Activation of Akt signaling is sufficient to maintain pluripotency in mouse and primate embryonic stem cells. Oncogene *25*, 2697–2707.

Watatani, Y., Ichikawa, K., Nakanishi, N., Fujimoto, M., Takeda, H., Kimura, N., Hirose, H., Takahashi, S., and Takahashi, Y. (2007). Stress-induced translation of ATF5 mRNA is regulated by the 5′-untranslated region. J. Biol. Chem. *283*, 2543–2553.

Williams, R.L., Hilton, D.J., Pease, S., Willson, T.A., Stewart, C.L., Gearing, D.P., Wagner, E.F., Metcalf, D., Nicola, N.A., and Gough, N.M. (1988). Myeloid leukaemia inhibitory factor maintains the developmental potential of embryonic stem cells. Nature *336*, 684–687.

Yen, P.H. (2004). Putative biological functions of the DAZ family. Int. J. Androl. *27*, 125–129.

Zong, Q., Schummer, M., Hood, L., and Morris, D.R. (1999). Messenger RNA translation state: the second dimension of high-throughput expression screening. Proc. Natl. Acad. Sci. USA *96*, 10632–10636.